Modeling organic aerosol concentrations and properties during winter 2014 in the northwestern Mediterranean region

Mounir Chrit[1], Karine Sartelet[1], Jean Sciare[2,3], Marwa Majdi[1,5], José Nicolas[2], Jean-Eudes Petit[2,4], and François Dulac[2]

[1]CEREA, joint laboratory Ecole des Ponts ParisTech - EDF R&D, Université Paris-Est, 77455 Champs sur Marne, France.
[2] LSCE, CNRS-CEA-UVSQ, IPSL, Université Paris-Saclay, Gif-sur-Yvette, France
[3] EEWRC, The Cyprus Institute, Nicosia, Cyprus
[4] INERIS, Parc Technologique ALATA, 60550 Verneuil-en-Halatte, France
[5] Laboratoire de Météorologie Dynamique (LMD)-IPSL, Sorbonne Université, CNRS UMR 8539, Ecole Polytechnique, Paris, France

Correspondence to: Mounir CHRIT (mounir.chrit@enpc.fr)

Abstract. Organic aerosols are measured at a remote site (Ersa) on Corsica Cape in the northwestern Mediterranean basin during the Chemistry-Aerosol Mediterranean Experiment (CharMEx) winter campaign of 2014, when high organic concentrations from anthropogenic origin are observed. This work aims at representing the observed organic aerosol concentrations and properties (oxidation state) using the air-quality model Polyphemus with a surrogate approach for secondary organic aerosol (SOA) formation. Because intermediate/semi-volatile organic compounds (I/S-VOCs) are the main precursors of SOA at Ersa during the winter 2014, different parameterizations to represent the emission and ageing of I/S-VOCs were implemented in the chemistry-transport model of Polyphemus (different volatility distribution emissions, single-step oxidation vs multi-step oxidation within a Volatility Basis Set framework, inclusion of non-traditional volatile organic compounds NTVOCs). Simulations using the different parameterizations are compared to each other and to the measurements (concentration and oxidation state). The high observed organic concentrations are well reproduced in all the parameterizations. They are slightly underestimated with most parameterizations. The volatility distribution at emissions influences more strongly the concentrations than the choice of the parameterization that may be used for ageing (single-step oxidation vs multi-step oxidation), stressing the importance of an accurate characterization of emissions. Assuming the volatility distribution of sectors other than residential heating to be the same as residential heating may lead to a strong under-estimation of organic concentrations. The observed organic oxidation and oxygenation states are strongly under-estimated in all simulations, even when multigenerational ageing of I/S-VOCs from all sectors is modeled. This suggests that uncertainties in the emissions and ageing of I/S-VOCs emissions remain to be elucidated, with a potential role of formation of organic nitrate and low-volatility highly oxygenated organic molecules.

1 Introduction

Organic aerosols (OA) are one of the main compound of submicron particulate matter (PM_1) (Jimenez et al., 2009). Their primary fraction originates mostly from combustion sources, such as traffic and residential heating. However, large uncertainties

remain regarding their emissions (Jathar et al., 2014; Gentner et al., 2017; Shrivastava et al., 2017; Tsimpidi et al., 2017). POA has been considered as non-volatile in emissions inventories and chemistry-transport models (CTMs); however, recent studies have provided clear evidence that a large portion of POA emissions partition between the gas and the particle phases (Robinson et al., 2007). Organic species that compose POA are often classified depending on their volatility: intermediate volatility organic compounds (IVOCs) (with saturation concentration C^* in the range 10^3-10^6 μg m^{-3}), semi-volatile organic compounds (SVOCs) (with saturation concentration C^* in the range 0.1-10^3 μg m^{-3}), or low-volatility organic compounds (LVOCs) (with saturation concentration C^* lower than 0.1 μg m^{-3}) (Lipsky and Robinson, 2006; Grieshop et al., 2009; Huffman et al., 2009; Cappa and Jimenez, 2010; Fountoukis et al., 2014; Tsimpidi et al., 2010; Woody et al., 2016; Ciarelli et al., 2017a, b).

OA originates not only from the partitioning of POA between the gas and the particle phases, but also from secondary aerosol formation (SOA) through the gas-to-particle partitioning of the oxidation products of biogenic and anthropogenic volatile organic compounds (VOCs) and intermediate and semi volatile organic compounds (I/S-VOCs). The main biogenic VOC precursors are terpenes (α-pinene, β-pinene, limonene, humulene) and isoprene (Shrivastava et al., 2017), while the main anthropogenic VOC precursors are aromatics (e.g. toluene, xylenes) (Dawson et al., 2016; Gentner et al., 2017).

Available measurements and modeling studies are useful to elucidate the composition and origin of OA in different seasons (Couvidat et al., 2012; Hayes et al., 2015; Canonaco et al., 2015; Chrit et al., 2017; Ciarelli et al., 2017b). Indeed, over the Mediterranean region, the oxidation of biogenic VOCs may dominate the formation of OA during the summer (El Haddad et al., 2013; Minguillón et al., 2016; Chrit et al., 2017). Chrit et al. (2017) found that I/S-VOC emissions do not influence much the concentrations of OA in summer over the Mediterranean region, but biogenic SOA prevail. Because biogenic emissions are low in winter, Canonaco et al. (2015) demonstrated a clear shift in the SOA origin between summer and winter during a measurement campaign from February 2012 to February 2013 conducted in Zürich using the Aerosol Chemical Speciation Monitor (ACSM, Ng et al. (2011)) measurements. This last study notably highlights the importance of biogenic VOC emissions and biogenic SOA production in summer, and the importance of residential heating in winter. Ciarelli et al. (2017a) performed a source apportionment study at the European scale and revealed that residential combustion (mainly related to wood burning) contributed about 60-70% to SOA formation during the winter whereas non-residential combustion and road-transportation sector contributed about 30-40% to SOA formation. Moreover, residential heating can also be a source of POA, which may make up a large fraction (20% to 90%) of the submicron particulate matter in winter (Murphy et al., 2006; May et al., 2013a; Denier van der Gon et al., 2015b; Shrivastava et al., 2017).

Modeling OA concentrations in winter is challenging, because it involves mostly the characterization of I/S-VOC emissions and ageing. Standard gridded emission inventories, such as those of the European Monitoring and Evaluation Programme (EMEP, www.emep.int) over Europe, do not yet include I/S-VOC emissions, and their emissions are still highly uncertain. For example, Denier van der Gon et al. (2015a) estimated that emissions from residential wood combustion were under-estimated by a factor 2-3 in the 2005 EUCAARI inventory. As an indirect method to account for the missing organic emissions in the absence of precise emission inventories, numerous modeling studies estimate the I/S-VOC emissions from POA emissions (Couvidat et al., 2012; Bergström et al., 2012; Koo et al., 2014; Zhu et al., 2016; Ciarelli et al., 2017a) or more recently from VOC emissions (Zhao et al., 2015, 2016; Ots et al., 2016; Murphy et al., 2017). A ratio of I/S-VOC/POA of 1.5 has been used

in several air quality studies (Bergström et al., 2012; Koo et al., 2014; Zhu et al., 2016; Ciarelli et al., 2017a). For example, Zhu et al. (2016) simulated the particle composition over Greater Paris during the winter MEGAPOLI campaign and they found that simulated OA agreed well with observed OA when gas-phase I/S-VOCs emissions are estimated using a ratio I/S-VOC/POA of 1.5, as derived following the measurements at the tailpipe of vehicles representative of the french fleet (Kim et al., 2016).

5 However, various ratios are used to better fit the measurements. For example, over Europe, Couvidat et al. (2012) used a ratio I/S-VOC/POA of 4 but also of 6 in a sensitivity simulation to better fit the observed OA concentrations in winter. Koo et al. (2014) used a ratio IVOC/POA of 1.5 but also of 3 in their high IVOC emission scenario.

The atmospheric evolution (also known as ageing) of I/S-VOCs as well as their impacts on atmospheric OA concentrations remain poorly characterized (Murphy et al., 2006) and deserve a better understanding. A widely used approach to model

10 the ageing of I/S-VOCs in CTMs is the volatility basis set (VBS) approach (Donahue et al., 2006). I/S-VOCs are divided into several classes of volatility where each class is represented by a surrogate. When oxidized by the hydroxyl radical, it leads to the formation of surrogates of lower volatility classes. This approach tends to lead to an overestimation of simulated organic concentrations (Cholakian et al., 2017) if fragmentation is not considered (formation of high volatility surrogates during the oxidation). Although the one-dimensional basis set 1-D VBS accounts for the volatility of the surrogates, it does not

15 allow the representation of varying oxidation levels of OA. The more powerful prognostic tool to date, bi-dimensional VBS approach (2D-VBS), although it is computationally burdensome, describes the ageing of I/S-VOCs using not only the volatility property (C^*) but also the oxidation level (the oxygen-to-carbon ratio O:C), taking into account three competing processes: functionalization, oligomerization and fragmentation (Donahue et al., 2012). Koo et al. (2014) developed a 1.5-D ageing VBS-type scheme that accounts for multigenerational ageing, including functionalization, oligomerization and fragmentation and

20 that represents both the volatility and the oxidation properties of the surrogates. When oxidized by a hydroxyl radical, each surrogate leads to the formation of more oxidized and less volatile surrogates with a reduced carbon number. Functionalization and fragmentation are implicitly taken into account in this approach, because of the increase of the oxygen number and the decrease of the carbon number of the surrogates formed. The 1.5-D VBS module is implemented within two widely used CTMs namely CAMx (ENVIRON, 2011) and CMAQ (Byun and Ching, 1999). Couvidat et al. (2012, 2013b, 2017) and Zhu et al.

25 (2016) used a simplified ageing scheme with 3 volatility bins. When oxidized by the hydroxyl radical, each surrogate forms a less volatile and more oxidized surrogate, that does not undergo multigenerational ageing. This simplified ageing scheme is implemented in the two widely used CTMs Polyphemus (Chrit et al., 2017) and Chimere (Couvidat et al., 2017).

In winter, when anthropogenic emissions impact the most air quality, anthropogenic emissions such as toluene and xylenes may also form SOA, although they may be much less efficient than I/S-VOCs (Couvidat et al., 2013a; Sartelet et al., 2018). To

30 take into account emissions and ageing of anthropogenic VOCs that are usually not considered in CTMs (phenol, naphtalene, m-,o-,p- cresol, etc.), Ciarelli et al. (2017b) modified the approach of Koo et al. (2014) by considering non traditional VOCs (NTVOCs). They are VOCs or IVOCs, not usually taken into account in CTMs, and with a saturation concentration in the low-range of IVOCs .

Following Bruns et al. (2016), Ciarelli et al. (2017b) estimated these NTVOCs, using chamber experiments, as the mixture of

35 phenol, m-, o-, p-cresol, m-, 15 o-, p-benzenediol/2-methylfuraldehyde, dimethylphenols, guaiacol/methylbenzenediols, naph-

thalene, 2-methylnaphthalene/1- methylnaphthalene, acenaphthylene, syringol, biphenyl/acenaphthene and dimethylnaphtha-lene. Furthermore, they estimated the ratio NTVOC/SVOC, where SVOC is the primary semi-volatile organic matter, to be about 4.75.

The oxidation level of OA is important, because it is indicative of the degree of hygroscopicity, surface tension (Jimenez
5 et al., 2009), and radiative property of the OA in addition to its ability to act as cloud condensation nuclei (CCN) over the Mediterranean (Jimenez et al., 2009; Duplissy et al., 2011; Wong et al., 2011). Chrit et al. (2017) showed that, in summer in the western Mediterranean region, OA is highly oxidized and oxygenated. The CTM Polyphemus/Polair3d used in their study does represent this high oxidation level of OA after adding to the model formation processes of highly oxidized species (autoxidation) and organic nitrate formation.

10 The particle oxidation state is represented by the organic mass to organic carbon ratio (OM:OC). According to Gilardoni et al. (2009) and Kroll et al. (2011), OM:OC is an index of the contribution of hetero-atoms (O, H, S, N, ...) to the organic mass: chemically processed and aged particles are expected to have higher OM:OC ratio compared to freshly emitted and unprocessed aerosols. The oxygenation state is represented by the oxygen to carbon ratio (O:C). It indicates the contribution of oxygen to organic molecules and the ability of carbon atoms to form bonds with oxygen.

15 Although the organic matter to organic carbon ratio (OM:OC) was first believed to lie between 1.2 and 1.4 (Grosjean and Friedlander, 1975), numerous studies (Turpin and Lim, 2001; El-Zanan et al., 2005; Aiken et al., 2008; Couvidat et al., 2012; Tost and Pringle, 2012; Canagaratna et al., 2015; Tsimpidi et al., 2018) show that OM:OC is rather close to 1.6 for urban aerosols and 2.1 for non urban aerosols. Zhang et al. (2005a) developed an algorithm to deconvolve the mass spectra of OA obtained with an Aerodyne^{TM} Aerosol Mass Spectrometer (AMS) in order to estimate the mass concentrations of hydrocarbon-
20 like and oxygenated organic aerosols (HOA and OOA). The mass of HOA represents primary sources, with a OM:OC ratio close to 1.2 and O:C ratio close to 0.1, while the mass of OOA represents secondary sources (aged and oxygenated) with a OM:OC ratio close to 2.2 and O:C ratio close to 1 (Aiken et al., 2008). Using this technique, Zhang et al. (2005b) found an average OM:OC ratio of 1.8 in Pittsburgh in September. Over Europe, Crippa et al. (2014) found that secondary OA is dominant in the OA fraction, with primary sources contributing to less than 30% to the total mass fraction. Xing et al. (2013) measured
25 a ratio OM:OC ratio over 14 cities throughout China and found that in summer, OM:OC is nearly 1.75 ± 0.13, while the ratio is lower in winter (1.59 ± 0.18). The OM:OC ratio is lower during winter due to the slow oxidation process owing to the low temperatures in addition the low biogenic contribution to OA mass during winter. At Ersa, over the Mediterranean during the summer, Chrit et al. (2017) found high OM:OC and O:C ratios (2.5 and 1 respectively). They are due to aged biogenic OA, which Chrit et al. (2017) were able to represent by adding the formation of extremely low-volatility species and organic nitrate
30 to the model and by considering the formation of organosulfate.

Quantifying the effect of I/S-VOC emissions and their impact on the atmospheric organic budget as well as the OA oxi-dation/oxygenation levels during different seasons is challenging in spite of the recent advances concerning the description of I/S-VOCs (Stockwell et al., 2015; Ciarelli et al., 2017b). This work aims at evaluating how commonly used parameteri-zations and assumptions of I/S-VOCs emissions and ageing perform to model the OA concentrations and properties in the

western Mediterranean region in winter. To that end, the CTM from the air quality platform Polyphemus is used with different parameterizations of I/S-VOCs emissions and ageing.

This paper is structured as follow: section 2 presents the setup of the air-quality model used and reference measurements. Section 3 presents the different emissions and ageing mechanisms used to describe the evolution of I/S-VOCs as well as the comparison method. Section 4 compares the simulated concentrations, compositions of OA for the simulations using the different parameterizations. Finally, section 5 compares the measured and simulated OM:OC and O:C ratios.

2   Model and measurement set-up

The period of interest of this study is January-March 2014, hereafter referred to as the winter 2014 campaign.

2.1   General model setup

The Polyphemus/Polair3d air-quality model is used, with a similar setup as Chrit et al. (2017). Transport, dry and wet deposition are modeled folowing Sartelet et al. (2007). The Carbon Bond 05 model is used for gas-phase chemistry. Semi-volatile organic compounds formation mechanisms from five SOA gaseous precursors namely isoprene, monoternenes, sesquiterpenes, aromatic compounds and intermediate and semi-volatile organic compounds from anthropogenic emissions (Kim et al., 2011; Couvidat et al., 2012) are added to CB05 model. Theses five precursors are modeled with a few surrogates as proxies to represent all the species. The aerosol dynamics (coagulation and condensation/evaporation) are modeled using the SIze REsolved Aerosol Model (SIREAM) (Debry et al., 2007) based on a sectional approach with an aerosol distribution of 24 sections of bound diameters: 0.01, 0.0141, 0.0199, 0.0281, 0.0398, 0.0562, 0.0794, 0.1121, 0.1585, 0.199, 0.25, 0.316, 0.4, 0.5, 0.63, 0.79, 1.0, 1.2589, 1.5849, 1.9953, 2.5119, 3.5481, 5.0119, 7.0795 and 10.0 μm.

The thermodynamic model used for condensation/evaporation of inorganic aerosol is ISORROPIA v1 (Nenes et al., 1998) and the gas/particle partioning of SOA is computed with SOAP (Couvidat and Sartelet, 2015). In order to compute the gas/particle partitioning of both inorganics and organics, a bulk equilibrium approach is adopted. After condensation/evaporation, the mass is redistributed among size bins using the moving diameter algorithm (Jacobson, 1997).

The simulations are run between 01 January and 02 April 2014 for both the nesting (Europe) and the nested (Mediterranean) domains. The simulation domains (Europe and Mediterranean) and the spatial resolution used in the present study are the same as the ones used in Chrit et al. (2017). The spatial resolutions used for the European and Mediterranean domains are $0.5° \times 0.5°$ and $0.125° \times 0.125°$ along longitude and latitude. 14 vertical levels are used for both domains from the ground to 12 km. The heights of the cell interfaces are 0, 30, 60, 100, 150, 200, 300, 500, 750, 1000, 1500, 2400, 3500, 6000 and 12 000 m.

Boundary conditions for the European domain are obtained from the global chemistry-transport model MOZART v4.0 (Horowitz et al., 2003) (https://www.acom.ucar.edu/wrf-chem/mozart.shtml). The European simulation provides initial and boundary conditions to the Mediterranean one. The European Center for Medium-Range Weather Forecasts (ECMWF) model provides the meteorological fields. The Troen and Mahrt parameterization (Troen and Mahrt, 1986) is used to compute the vertical diffusion. The land cover is modeled using the Global Land Cover 2000 (GLC-2000; http://www.gvm.jrc.it/glc2000/) data

set. Sea-salt emissions are parameterized following Jaegle et al. (2011) and are assumed to be composed of sodium, chloride and sulfate (Schwier et al., 2015). Biogenic emissions are estimated with the Model of Emissions of Gases and Aerosols from Nature (MEGAN, Guenther et al. (2006)). Anthropogenic emissions are generated using the EDGAR-HTAP_V2 inventory for 2010 (http://edgar.jrc.ec.europa.eu/htap_v2/). The monthly and daily temporal distribution for the different activity sectors

5   are obtained from GENEMIS (1994), and the hourly temporal distribution from Sartelet et al. (2012). NO_x, SO_x and $PM_{2.5}$ emissions are speciated as described in Chrit et al. (2017). I/S-VOC gas-phase emissions are estimated from the POA emissions from residential heating by multiplying them by a constant factor assumed to be 1.5 in the default simulation. The total (gas + particle) I/S-VOC is therefore equal to 2.5 the original POA.

As described in section 3.5, different values will be used and compared for I/S-VOC gas-phase emissions from residen-
10   tial heating and from other sectors. The I/S-VOCs emissions from residential heating are assumed to be those of the sector "htap_6_residential" of the EDGAR-HTAP_V2 inventory. The emissions from this sector (shown in Figure 1) concern the emissions from heating/cooling and equipment/lightening of buildings as well as waste treatment. The I/S-VOC emissions from residential heating are obtained from the POA emissions of sector 6 by multiplying them by a constant factor noted R_{RH} = I/S-VOC/POA. These emissions over the Mediterranean domain are located over big cities (Marseille, Milan, Rome, etc).
15   I/S-VOC emissions from the six other anthropogenic sources (shown in Figure 1) are estimated from the POA emissions by multiplying them by a constant factor noted R = I/S-VOC/POA. These emissions are located over big cities and along the main traffic routes, as well as the shipping routes linking Marseille to Ajaccio and Bastia. Different estimations of R and R_{RH} will be used, as well as different approaches to represent the ageing of I/S-VOCs (section 3).
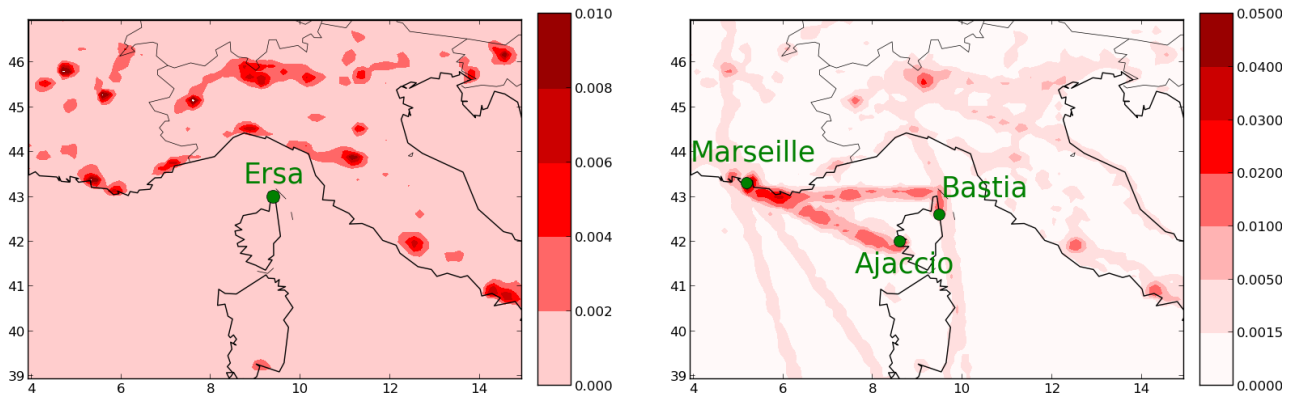
Figure 1. Surface emissions of POA from the residential heating sector (left panel) and from the other six anthropogenic sectors (right panel) during the winter 2014. The emissions are in $\mu g.m^{-2}.s^{-1}$

2.2 Measurement setup

The ground-based measurements were performed in the framework of ChArMEx (The Chemistry-Aerosol Mediterranean Experiment) at Ersa (42°58'N, 9°21.8'E) on a ridge at the northern tip of Corsica Island at an altitude of about 530 m.a.s.l.. The ground-based comparisons are performed by comparing the measured and modeled concentrations at the model cell closest to the station (42°52N, 9°22'30"E, 494 m.a.s.l.), as detailed in Chrit et al. (2017). An Aerodyne^{TM} ACSM was used in order to measure the near real-time mass concentration and chemical composition of aerosols with aerodynamic diameters between 70 and 1000 nm with a time resolution of 30-min (Ng et al., 2011). This instrument has been continuously running at Ersa between June 2012 and July 2014 (Nicolas, 2013), with an on-site set-up similar to the one presented in Michoud et al. (2017). A recent intercomparison exercise, in which the ACSM used in this study has successfully taken part, reports an expanded uncertainty of 19% for OM (Crenn et al., 2015). OM:OC and O:C ratios are estimated using these measurements following the methodology provided in Kroll et al. (2011). Although Crenn et al. (2015) and Fröhlich et al. (2015) have shown consistent results (e.g. satisfactorily Z-scores) in terms of fragmentation pattern, higher discrepancies were observed for f_{44} (mass fraction of m/z44), which is an essential variable in the calculation of these elemental ratios. In this respect, results are presented with an uncertainty which can be estimated as being twice the one of PM (i.e. around 40%). The measurements are compared to concentrations and properties of particles of diameters between 0.01 and 1 μm.

2.3 Model/measurements comparison method

To evaluate the performance of the model, we compare model simulation results to measurements at the Ersa site using a variety of performance statistical indicators. These indicators are: the simulated mean ($\bar{s}$), the root mean square error (RMSE), the correlation coefficient (corr), the mean fractional bias (MFB) and the mean fractional error (MFE). Table A1 of Appendix A lists the key statistical indicators definitions used in the model-to-data intercomparison. Furthermore, the criteria of Boylan and Russell (2006) (detailed in Table A2 of Appendix A) is used to assess the performance of the simulations.

3 Modeling of I/S-VOC emissions and ageing

In order to understand the behavior of the different parameterizations commonly used in CTMs to represent emissions and ageing of I/S-VOCs in the western Mediterranean region, several simulations using different parameterizations, described in the following sections, are compared. These parameterizations are those described in Couvidat et al. (2012), Koo et al. (2014) and Ciarelli et al. (2017b). The differences concern the emission ratios used to estimate I/S-VOCs from POA (R and R_{RH}), the ageing scheme (one step or multi-generational), the modeling of NTVOCs, as well as the ratio OM:OC and volatility distribution at emissions.

3.1 One-step oxidation scheme

The one-step oxidation mechanism of Couvidat et al. (2012) is based on the fitting of the curve of dilution of POA from diesel exhaust of Robinson et al. (2007). I/S-VOCs are modeled with three surrogate species POAlP, POAmP and POAhP of different volatilities chosen to fit the dilution curve of POA from diesel exhaust of Robinson et al. (2007) and characterized by their

5 saturation concentrations (0.91, 86.21 and 3225.80 μg m^{-3} respectively). The properties of the primary and aged I/S-VOCs are shown in Table B1 of Appendix B. The ageing of each of these primary surrogates is modeled by a one-step OH-oxidation reaction in the gas phase (Appendix B), leading to the formation of secondary surrogates SOAlP, SOAmP and SOAhP. Once formed, these secondary surrogates do not undergo further oxidations. Compared to the primary surrogates, the volatility of the secondary surrogates is reduced by a factor of 100 and their molecular weight is increased by 40% (Grieshop et al., 2009;

10 Couvidat et al., 2012) to represent functionalization and fragmentation.

3.2 Multi-generational step oxidation scheme

In sensitivity simulations, for anthropogenic I/S-VOC emissions, the oxidation mechanism is based on the hybrid volatility basis set (1.5-D VBS) approach developed by Koo et al. (2014). This mechanism combines the simplicity of the 1-dimensional (1-D) VBS with the ability to describe evolution of OA in the 2-dimensional space of oxidation state and volatility. This

15 basis set uses five volatility surrogates, characterized by saturation concentrations varying between 0.1 and 1000 μg m^{-3}. The surrogates VAP0, VAP1, VAP2, VAP3 and VAP4 refer to the primary surrogates and VAS0, VAS1, VAS2, VAS3 and VAS4 refer to the secondary ones. Table C1 of Appendix C lists their properties.

In the scheme developed by Koo et al. (2014), the OH-oxidation of the primary surrogates leads to a mixture of primary and secondary surrogates of lower volatility. The carbon (oxygen respectively) number of the lower volatility surrogate decreases

20 (increases respectively) indicating that functionalization and fragmentation are implicitly accounted for. This mechanism is detailed in Appendix C.

3.3 Multi-generational step oxidation scheme for residential heating

In sensitivity simulations, for anthropogenic I/S-VOC emissions from residential heating, the VBS model developed by Ciarelli et al. (2017b) is also used. As in the previously detailed multi-step oxidation scheme, five surrogates with volatilities characterized by saturation concentrations extending from 0.1 to 1000 μg m^{-3} are used. The primary surrogates (BBPOA1,

25 BBPOA2, BBPOA3, BBPOA4, BBPOA5) react with OH to form secondary surrogates (BBSOA0, BBSOA1, BBSOA2, BB-SOA3, BBSOA4), whose volatility is one order of magnitude lower than the primary surrogate. In opposition to the one-step and multi-step oxidation schemes detailed above, here the secondary surrogates may also undergo OH-oxidation forming the secondary surrogate of lower volatility. As in the other schemes, functionalization and fragmentation are taken into account as

30 the carbon and oxygen numbers of the secondary surrogates decreases and increases respectively. The properties of the VBS surrogates are shown in Table D1 of Appendix D, where reactions are also detailed.

Data from recent wood combustion and ageing experiments performed in smog chamber by Ciarelli et al. (2017b) show significant contribution of SOA from non-traditional volatile organic compounds (NTVOCs: phenol, m-, o-, p-cresol, m-, o-, p-benzenediol/2-methylfuraldehyde, dimethylphenols, guaiacol/methylbenzenediols, naphthalene, 2-methylnaphthalene/1-methylnaphthalene, acenaphthylene, syringol, biphenyl/acenaphthene, dimethylnaphthalene) to OA mass. These NTVOCs are usually not accounted as SOA precursors in CTMs. The NTVOC mixture saturation concentration is estimated to be $\sim 10^6$ μg m^{-3} falling with the IVOC saturation concentrations range limit (Koo et al., 2014; Donahue et al., 2012). NTVOCs emissions are estimated using a ratio of NTVOC/SVOC of 4.75 (Ciarelli et al., 2017b) and their OH-oxidation produces four secondary surrogates of different volatilities. These four surrogates may undergo OH-oxidation leading to the less volatile and more oxidized secondary surrogate, similarly to the multi-step oxidation described in section 3.3. This mechanism is detailed in Appendix D and the surrogates properties are listed in Table D1 of Appendix D.

3.4 Volatility distribution and properties of primary emissions

Table 1 shows emission rates of OA precursors averaged over the Mediterranean domain and over the simulation period.

OA precursor	Emission rate (μg.m^{-2}s^{-1})
VOCs from biogenic and anthropogenic sources	0.0314
NTVOCs	0.0062
I/S-VOCs from residential heating	0.0013
I/S-VOCs from other sources	0.0030

Table 1. Emission rates of OA precursors averaged temporally and over the Mediterranean domain.

Emissions of I/S-VOCs are allocated into the surrogate compounds detailed in the above sections using emission distribution profiles, which are based on chamber measurements. The distribution of the emission profiles as a function of volatility (saturation concentration) is detailed in Table 2. Two emission profiles are used. The first one corresponds to the measurements of May et al. (2013b) for biomass burning, and it is similar to the emission profile used by Couvidat et al. (2012) for all sectors and by Ciarelli et al. (2017b) for residential heating. The second emission profile corresponds to an average of emission distributions from gasoline and diesel vehicles measured by May et al. (2013c, d), and it is used in Koo et al. (2014). Here, the volatility emission distributions are assigned to a profile number (equal to 1 or 2), depending on whether the volatility profile is similar to the profile from biomass burning emissions of May et al. (2013c) (profile number 2) or whether it is similar to the profile from vehicle emissions of May et al. (2013d) and May et al. (2013b) (profile number 1). As shown in Table 2, the emitted I/S-VOCs are less volatile in the profile 1 than in the biomass-burning volatility distribution (profile 2). Depending on the emission sector, the OM:OC and O:C ratios of the emitted surrogates may differ. For most sectors, such as traffic, the OM:OC and O:C ratios are assumed to be low (OM:OC is equal to 1.3 in Couvidat et al. (2012). However, for residential heating, the emissions may be more oxidized. The scheme of Ciarelli et al. (2017b) assumes higher OM:OC and O:C rations, as described in Table 3. Here, the OM:OC and O:C ratios are assigned to a profile number (equal to 1 or 2), depending on

Profil N°	1	2		1	2
Reference	May et al. (2013c, d)	Couvidat et al. (2012)		May et al. (2013c, d)	May et al. (2013b)

Saturation Conc.			Saturation Conc.		
0.9	0.35 [POAlP]	0.25 [BBPOAlP]	0.1	0.15 [VAP0]	0.20 [BBPOA0]
			1	0.20 [VAP1]	0.10 [BBPOA1]
86.2	0.51 [POAmP]	0.32 [BBPOAmP]	10	0.31 [VAP2]	0.10 [BBPOA2]
			100	0.20 [VAP3]	0.20 [BBPOA3]
3225.8	0.14 [POAhP]	0.43 [BBPOAhP]	1000	0.14 [VAP4]	0.4 [BBPOA4]

Table 2. Summary of the volatility distributions of the primary I/S-VOC surrogates. Saturation concentrations are expresssed in μg m^{-3}. For each saturation concentration and volatility coefficient, the name of the associated primary surrogate is between two square brackets.

Profil N°	1	2		1	2
Reference	Couvidat et al. (2012)			Koo et al. (2014)	Ciarelli et al. (2017b)

Saturation Conc.			Saturation Conc.		
0.9	1.3 (0.15) [POAlP]	1.7 (0.55) [BBPOAlP]	0.1	1.36 (0.16) [VAP0]	1.64 (0.37) [BBPOA0]
			1	1.31 (0.12) [VAP1]	1.53 (0.29) [BBPOA1]
86.2	1.3 (0.15) [POAmP]	1.7 (0.55) [BBPOAmP]	10	1.26 (0.07) [VAP2]	1.44 (0.22) [BBPOA2]
			100	1.21 (0.03) [VAP3]	1.36 (0.15) [BBPOA3]
3225.8	1.3 (0.15) [POAhP]	1.7 (0.55) [BBPOAhP]	1000	1.17 (0) [VAP4]	1.28 (0.09) [BBPOA4]

Table 3. Summary of the OM:OC (and O:C) ratio of the primary I/S-VOC surrogates. Saturation concentrations are expresssed in μg m^{-3}. For each saturation concentration and OM:OC ratio, the name of the associated primary surrogate is between two square brackets.

whether the ratios are similar to the profile from biomass burning emissions of Ciarelli et al. (2017b) (profile number 2) or whether they are lower (profile number 1).

3.5 Sensitivity simulations

The setup of the different simulations is summarized in Table 4. The simulation S1 uses the setup commonly used in air-quality simulations with the Polyphemus platform: the one-step ageing scheme of Couvidat et al. (2012) is used for both residential heating and other anthropogenic sectors.

The links between the compared simulations and the sensitivity parameters studied are summarized in Table 5. The simulation S2 is conducted to evaluate the impact of the volatility distribution of emissions. Instead of using a volatility distribution specific of biomass burning for all sectors as in S1, the volatility distribution specific of car emissions is used for anthropogenic sectors other than residential heating.

The simulation S3 is conducted to evaluate the impact of the ageing scheme. The volatility distributions are similar as S2, but multi-generational schemes are used rather than a single-oxidation strep for all anthropogenic sectors.

Simulation	Residential heating					Other anthropogenic sectors			
	Ageing	Volatility profile	R_{RH}	OM:OC profile	NTVOCs	Ageing	Volatility profile	R	OM:OC profile
S1	one-step (Couvidat)	2	1.5	1	No	one-step (Couvidat)	2	1.5	1
S2	one-step (Couvidat)	2	1.5	2	No	one-step (Couvidat)	1	1.5	1
S3	multi-step (Ciarelli)	2	1.5	2	No	multi-step (Koo)	1	1.5	1
S4	multi-step (Ciarelli)	2	1.5	2	Yes	multi-step (Koo)	1	1.5	1
S5	one-step (Couvidat)	2	4.0	2	No	one-step (Couvidat)	1	1.5	1
S6	multi-step (Ciarelli)	2	4.0	2	Yes	multi-step (Koo)	1	1.5	1

Table 4. Summary of the parameters used in the different simulations performed.

Sensitivity study of the impact of	Simulations to be compared
the volatility distribution of emissions	S1, S2
the ageing scheme	S3, S2
NTVOCs	S4, S2
the I/S-VOC/POA ratio	S5, S2 and S6,S4

Table 5. Links between the compared simulations and the sensitivity parameters studied.

The simulation S4 is evaluated to estimate the impact of NTVOCs. It has the same setup as S2 with multi-generational ageing, but NTVOCs are taken into account. Even though NTVOCs are added, emissions of I/S-VOCs as modeled by the factor R_{RH} are kept.

The simulations S5 and S6 are conducted to assess the impact of the I/S-VOC/POA ratio used for residential heating (R_{RH}). The simulation S5 has the same setup as the simulation S2 (single-step oxidation), but it differs in the ratio R_{RH}, which is assumed to be equal to 4 rather than 1.5. The simulation S6 has the same setup as the simulation S4 (multi-step oxidation and NTVOCs), but it differs in the ratio R_{RH}, which is assumed to be equal to 4 rather than 1.5.

In terms of the OM:OC ratio, the ratio specific of car emissions is used for emissions from anthropogenic sectors other than residential heating. For residential heating, higher OM:OC ratios are used in all simulations, except in S1, where the ratio specific of car emissions is used for all sectors.

4 Organic concentrations

The spatial distribution of OM_1 concentrations averaged over the first 3 months of 2014 (Figure E1 of Appendix E) shows that high OM_1 concentrations are mostly located over big cities like Marseille (2.0 μg.m^{-3}), Genoa (1.6 μg.m^{-3}), Turin (4.3 μg.m^{-3}), Milan (4.4 μg.m^{-3}), Rome (2.4 μg.m^{-3}) and Naples (2.1 μg.m^{-3}) and along maritime traffic routes, stressing that organics during wintertime are likely to be mostly of anthropogenic origins.

The simulated composition of OM_1 at Ersa is shown in Figure 2 for the simulations S4 and S5. In all simulations, primary and secondary organic aerosols (POA and SOA) from anthropogenic I/S-VOCs are the main components of the organic mass (between 60% and 84%). POA tends to account for almost the same fraction of the organic mass than SOA (between 46% and 62%). Similarly, in the U.S., Koo et al. (2014) found that the SOA account for less than half of the modeled OA mass in winter 2005 due to the slow chemical ageing during the cold season. Over Europe, in March 2009, Ciarelli et al. (2017a) simulated that POA accounts between 12 and 68% of the OA, with an average value of 38%. The emission sector 6 (residential heating) has a large contribution to OA (between 31% and 33%). This is also in line with Ciarelli et al. (2017a) who found that over Europe in March 2009, the contribution of the residential sector to OA varies between 20% and 45% with an average value of 38%. Furthermore, this sector contributes more to SOA (between 42% and 52% of SOA from I/S-VOCs) than to POA (between 17% and 31% of POA from I/S-VOCs), because their I/S-VOC emissions are more volatile. The contribution from aromatic VOCs is low (lower than 3%), and when NTVOCs are considered, they represent between 18% and 21% of the organic mass. The model simulations performed revealed that, for the winter 2014, the biogenic OA fraction is low (15-18%). Ciarelli et al. (2017a) also estimated the biogenic contribution to the organic budget to be between 5 and 20% over Europe.
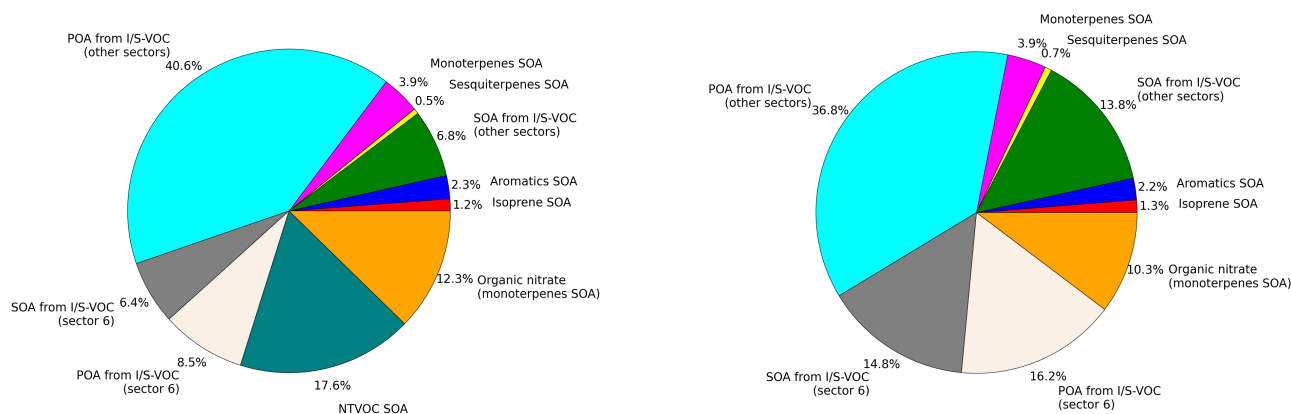
Figure 2. Simulated composition of OM_1 during the winter campaign of 2014 for two simulations: S4 (left panel) and S5 (right panel).

The statistical evaluation of the simulations is shown in Table 6. The model-to-measurement correlation is high for all simulations (between 76 and 83%). The performance criterion is satisfied for all simulations and the goal criterion is satisfied for S2, S3, S4 and S5. The goal criterion is not satisfied for the simulation S1, which uses single-step oxidation with a biomass-burning type volatility distribution for all anthropogenic sectors, and for the simulation S6, which uses multi-step oxidation with NTVOCs and a high R_{RH} ratio. The simulation S1 strongly under-estimates the OM_1 concentration at Ersa, whereas the simulation S6 strongly over-estimates it. All the simulations tend to under-estimate the OM_1 concentrations at Ersa, except for the two simulations where NTVOCs are taken into account (S4 and S6), which over-estimate the OM_1 concentrations at Ersa. Because I/S-VOC emissions as modeled by the factor R_{RH} are kept in those simulations, the IVOCs forming SOA may have been counted twice by adding NTVOCs, explaining the over-estimation.

Simulations	S1	S2	S3	S4	S5	S6
$\overline{s} \pm$ RMSE	0.75 ± 1.14	1.06 ± 0.91	1.20 ± 0.85	1.65 ± 0.79	1.25 ± 0.80	2.06 ± 1.08
Correlation (%)	78.3	76.7	76.2	82.4	78.8	82.7
MFB (%)	-55	-23	-11	17	-7	38
MFE (%)	59	40	37	39	35	48

($\overline{o} = 1.45$)

Table 6. Statistics of model to measurements comparisons for daily OM_1 concentrations during the winter campaign of 2014 at Ersa. $\overline{o}$ refers to the observed mean. Other statistical indicators are defined in Table A1 of AppendixA.

Other CTMs showed the same under-estimation of OM_1 concentrations during winter over Europe, even when I/S-VOC emissions are taken into account (Couvidat et al., 2012; Denier van der Gon et al., 2015a). The CTM CAMx (Comprehensive Air Quality Model with extensions) also under-estimated the organic concentrations over Europe during February and March 2009 (Ciarelli et al., 2017a), but considerable improvement was found for the modeled OA mass with the MFB decreasing from -61 to -29 %, when the parameterization of Ciarelli et al. (2017b) with NTVOCs was added.

The model-to-measurement comparison during the first three months of 2014 in terms of the daily concentrations of OM_1 at Ersa is shown in Figure 3. Globally, the temporal variations of the simulated concentrations are well reproduced by the model. The simulation S1, which uses single-step oxidation with a biomass-burning type volatility distribution for all anthropogenic sectors, under-estimates the peaks. However, the peaks are well reproduced by the simulations S2, S3 and S5. The simulations S4 and S6, which take into account NTVOCs over-estimate the peaks. All simulations under-estimate the beginning of the peak between 9 and 15 March, probably due to uncertainties in meteorology especially rain episodes, and changes in the origin of air masses.
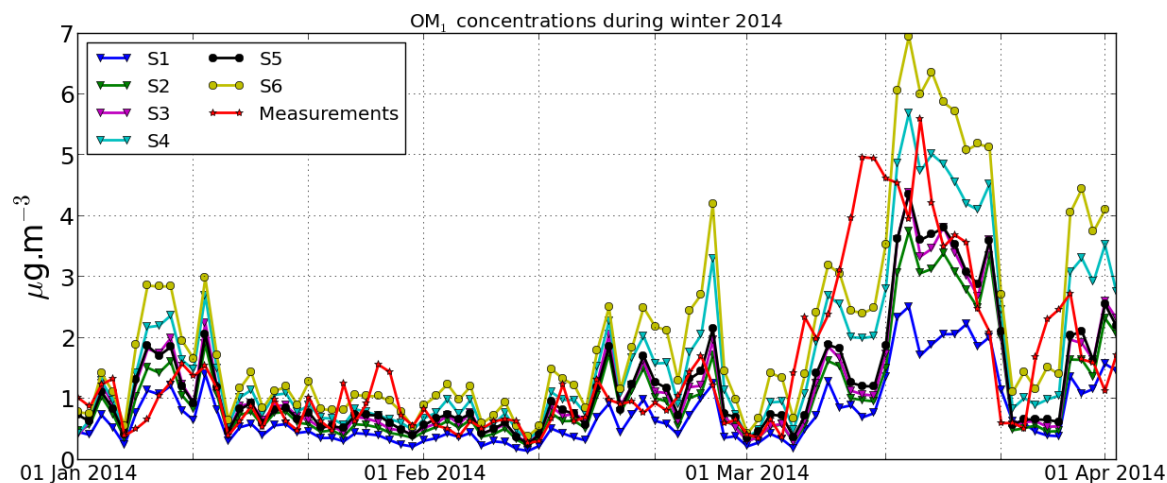
Figure 3. Daily evolution of measured and simulated OM_1 concentrations at Ersa from 1 January to 2 April.

As detailed in section 3.5, the differences between the simulations S2 and S1 originate in differences in the volatility distribution of emissions from anthropogenic sectors other than residential heating. In the simulation S2, a less volatile distribution is used than in the simulation S1, leading to larger OA concentrations in the particle phase. This difference in the volatility distribution makes a large difference in the OA concentrations, removing the strong under-estimation simulated in simulation S1 (the MFB is -55% in S1 and only -23% in S2).

Considering multi-step ageing for all anthropogenic sectors also leads to an increase of OA concentrations (the MBF of the simulation S3 is -11%, which is lower in absolute value than the simulation S2). However, the influence of the multi-step ageing (difference between S2 and S3 shown in Figure E1 of Appendix E) is lower than the influence of the volatility distribution (difference between S1 and S2 shown in Figure E1 of Appendix E). This larger influence of the volatility distribution than the multi-step ageing is true not only at Ersa, but also over the whole Mediterranean domain, where the average RMSE between the simulations S1 and S2 is 0.01 μg m^{-3} (impact of volatility), against 0.005 μg m^{-3} for the RMSE between the simulations S2 and S3 (impact of multi-step ageing).

At Ersa, increasing the ratio R$_{RH}$ from 1.5 to 4 (difference between simulation S3 and S2 shown in Figure E1 of Appendix E) has almost the same impact as considering the multi-step ageing (difference between simulations S5 and S2 shown in Figure E1 of Appendix E), although the statistics are slightly better when the ratio R$_{RH}$ is increased from 1.5 to 4 than when multi-step ageing is considered. However, this is not true over the whole Mediterranean domain, where the impact of increasing the ratio R$_{RH}$ from 1.5 to 4 is large over cities, whereas the impact of multi-step ageing stays low (see Figure E1 of Appendix E). Over the whole Mediterranean domain, the average RMSE between the simulations S2 and S5 is 0.014 μg m^{-3} (impact of increasing the ratio R$_{RH}$ from 1.5 to 4), against 0.005 μg m^{-3} for the RMSE between the simulations S2 and S3 (impact of multi-step ageing).

Finally, the best statistics, in terms of MFE and MFB are obtained for the simulation S5, with a one-step ageing scheme, a volatility distribution typical of biomass burning for the residential sector with a ratio R$_{RH}$ of 4, and a volatility distribution typical of car emissions for other sectors with a ratio R of 1.5.

5 Oxidation and oxygenation of organics

The oxidation state is quantified using two metrics: OM:OC and O:C calculated as detailed in Chrit et al. (2017). Figure 4 shows the daily variations of the measured and simulated ratios for the different simulations.
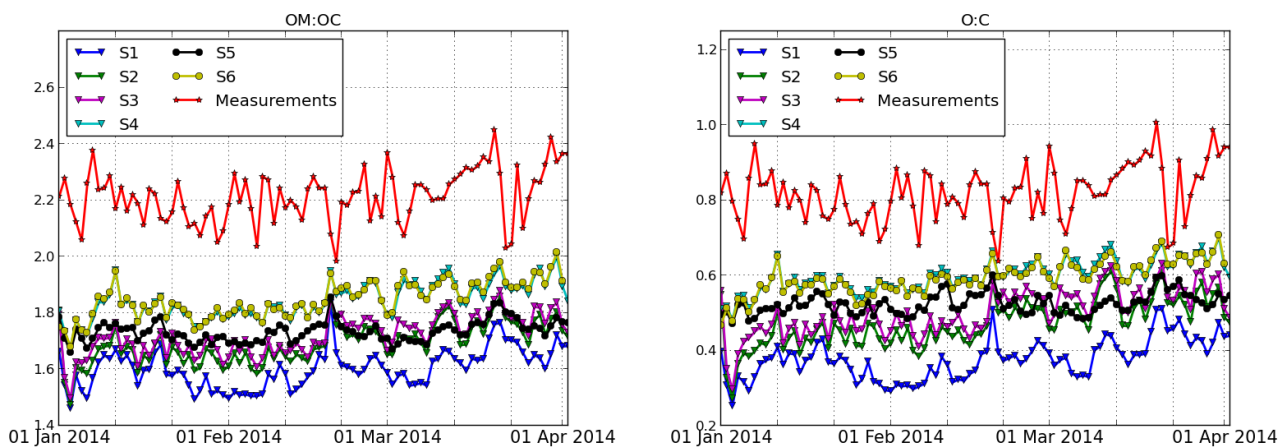
Figure 4. Daily evolution of the ratios OM:OC (left panel) and O:C (right panel) from 01 January to 02 April 2014 at Ersa.

The measurements at Ersa show highly oxidized and oxygenated organics: the measured OM:OC and O:C ratios at Ersa are respectively 2.21 ± 0.09 and 0.82 ± 0.07 These values are lower than the index measured during the summer 2013 by Chrit et al. (2017) (2.43 ± 0.07 and 0.99 ± 0.06 for the measured OM:OC and O:C ratios at Ersa respectively), due to the slower oxidation process owing to the lower temperatures during winter. The average simulated OM:OC and O:C ratios are shown in Table 7. Both index are strongly underestimated by all simulations, due to the high contribution of POA to the OM_1 concentrations (POA is less volatile and oxygenated than SOA). The simulations using multi-step ageing schemes for I/S-VOC emissions have higher OM:OC and O:C ratios, although the differences are very low (the OM:OC ratio is 1.69 ± 0.53 in S2 (single-step) and 1.72 ± 0.50 in S3 (multi-step). Organics in the simulations where the strength of I/S-VOC emission from residential heating was increased (simulations S5 and S6) have higher OM:OC and O:C ratios because POA and SOA from I/S-VOCs from residential heating are more oxidized and oxygenated than POA and SOA from other anthropogenic sources. Similarly, organics in the simulations where NTVOCs are taken into account have higher OM:OC and O:C ratios, because in the model, NTVOCs lead to very oxidized and oxygenated OA. However, the simulated ratios OM:OC and O:C stay under-estimated (1.85 ± 0.38 and 0.60 ± 0.24 at most, against 2.21 ± 0.09 and 0.82 ± 0.07 in the measurements).

Simulations	S1	S2	S3	S4	S5	S6	Measurements
OM:OC	1.60 ± 0.62	1.69 ± 0.53	1.72 ± 0.50	1.85 ± 0.38	1.74 ± 0.49	1.85 ± 0.38	2.21 ± 0.09
O:C	0.38 ± 0.45	0.47 ± 0.36	0.50 ± 0.33	0.60 ± 0.23	0.53 ± 0.31	0.59 ± 0.24	0.82 ± 0.07

Table 7. Daily averages of OM:OC and O:C ratios at Ersa during winter 2014 for the different simulations. The average measured OM:OC ratio is 2.21 and the average measured O:C ratio is 0.82.

The underestimation of the O:C ratio may be due to an underestimation of oxidants' concentrations and secondary aerosol formation. Figure 5 shows that the model tends to underestimate ozone concentrations (the modeled and measured average concentrations between 21 January and 24 February 2014 are 46.2 and 68.0 μg.m^{-3}). However, the O:C ratio stays underestimated even during the days where ozone is well modeled. It is difficult to conclude on the underestimation of oxidants, because measurements were not performed for other oxidants than ozone, such as OH, which probably has other sources than ozone photolysis in winter.
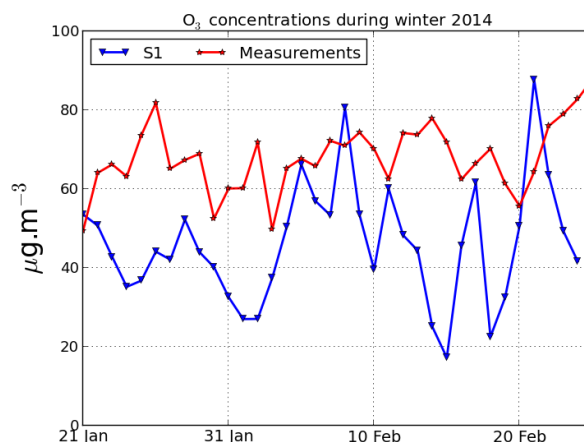
Figure 5. Daily evolution of ozone concentrations from 21 January to 24 February 2014 at Ersa.

6 Conclusion

This study shows a ground-based comparison of both modeled organic concentrations and properties to measurements performed at Ersa (Cape Corsica, France) during the winter 2014. This work aims at evaluating how commonly used parameterizations and assumptions of intermediate/semi-volatile organic compound (I/S-VOC) emissions and ageing perform in modeling OA concentrations and properties in the western Mediterranean region in winter. To that end, the chemistry-transport model from the air quality platform Polyphemus is used with different parameterizations of I/S-VOC emissions and ageing (different volatility distribution emissions, single-step oxidation vs multi-step oxidation within a Volatility Basis Set framework, including non-traditional volatile organic compounds NTVOCs). Winter 2014 simulations are performed and compared to measurements obtained with an ACSM at the background station of Ersa in the North of Corsica Island. In all simulations, OA at Ersa is mainly from anthropogenic sources (only 15 to 18% of OA is from biogenic sources). The emission sector 6 (residential heating) has a large contribution to OA (between 31 and 33%). The contribution from aromatic VOCs is low (lower than 3%). NTVOCs, as modeled with the parameterization of Ciarelli et al. (2017b) represent between 18% and 21% of the organic mass. For most simulations, the concentrations of OA compare well to the measurements.

Over the whole western Mediterranean domain, the volatility distribution at the emission influences more strongly the concentrations than the choice of the parameterization that may be used for ageing (single-step oxidation vs multi-step oxidation). Modifying the volatility distribution of sectors other than residential heating leads to a decrease of 29% in OA concentrations at Ersa, while using the multi-step oxidation parameterization rather than the single-step one leads to an increase of 13%. The best statistics are obtained using two configurations: the first one is a one-step ageing scheme, a volatility distribution typical of biomass burning for the residential sector with a ratio I/S-VOC/POA at emission of 4, and the second one is a multi-generational ageing scheme, a volatility distribution typical of car emissions for other sectors with a ratio R I/S-VOC/POA at emission of 1.5.

Both the OM:OC and O:C ratios are underestimated at Ersa in all simulations. The largest simulated OM:OC ratio is equal to 1.85 ± 0.83, against 2.21 ± 0.09 in the measurements. For the summer campaign, Chrit et al. (2017) improved the simulated OM:OC ratio by adding the formation mechanisms of extremely-low volatile organic compounds from the autoxidation of monoterpenes and organic nitrate from monoterpene oxidation. Similarly, the formation of organic nitrate and highly oxygenated organic molecules (Molteni et al., 2018) from the autoxidation of aromatic precursors should be added in order to better reproduce the observed OA oxidation/oxygenation levels.

However, adding these new OA formation pathways may lead to an increase in OA concentrations, suggesting that the actual parameterizations may need to be revisited, for example by better characterizing their deposition. Because the volatility distribution at the emission is the parameter influencing the most the concentrations, further experimental research should therefore focus on characterizing it for the different sectors. The emissions and formation of very low-volatility compounds should also be further investigated to represent the aerosol characteristics observed.

Acknowledgements. This research was funded by the French National Research Agency (ANR) projects SAF-MED (grant ANR-12-BS06-0013). It is part of the ChArMEx project supported by ADEME, CNRS-INSU, CEA and Météo-France through the multidisciplinary programme MISTRALS (Mediterranean Integrated Studies aT Regional And Local Scales). It contributes to ChArMEx work packages 1 and 2 on emissions and aerosol ageing, respectively. The ACSM at Ersa was funded by the CORSiCA project funded by the Collectivité Territoriale de Corse through the Fonds Européen de Développement Régional of the European Operational Program 2007-2013 and the Contrat de Plan Etat-Région. Eric Hamounou is acknowledged for his great help in setting up the Ersa station. We thank François Gheusi for the measurements of ozone concentrations. CEREA is a member of the Institut Pierre-Simon Laplace (IPSL).

References

Aiken, A., DeCarlo, P., Krol, J., Worsno, D., Huffma, J., Docherty, K., Ulbrich, I., Mohr, C., Kimmel, J., Sueper, D., Sun, Y., Zhang, Q., Trimborn, A., Northway, M., Ziemann, P., Canagaratna, M., Onasch, T., Alfarra, M., Prevot, A., Dommen, J., Duplissy, J., Metzger, A., Baltensperger, U., and Jimenez, J.: O/C and OM/OC Ratios of Primary, Secondary, and Ambient Organic Aerosols with High-Resolution Time-of-Flight Aerosol Mass Spectrometry., Environ. Sci. Technol., 42, 4478–4485, doi:10.1021/es703009q, 2008.

Bergström, R., Denier van der Gon, H., Prévôt, A., Yttri, K., and Simpson, D.: Modelling of organic aerosols over Europe (2002-2007) using a volatility basis set (VBS) framework: application of different assumptions regarding the formation of secondary organic aerosol., Atmos. Chem. Phys., 12, 8499–8527, doi:10.5194/acp-12-8499-2012, 2012.

Boylan, J. W. and Russell, A. G.: PM and light extinction model performance metrics, goals, and criteria for three-dimensional air quality models, Atmos. Environ., 40, 4946–4959, doi:10.1016/j.atmosenv.2005.09.087, 2006.

Bruns, E. A., El Haddad, I., Slowik, J. G., Kilic, D., Klein, F., Baltensperger, U., and Prévôt, A. S. H.: Identification of significant precursor gases of secondary organic aerosols from residential wood combustion, Sci. Rep., 6, 27 881, doi:10.1038/srep27881, 2016.

Byun, D. and Ching, J.: Science algorithms of the EPA Models-3 Community Multiscale Air Quality (CMAQ) Modeling System, environmental Protection Agency, Research Triangle Park, NC, 1999.

Canagaratna, M. R., Jimenez, J. L., Kroll, J. H., Chen, Q., Kessler, S. H., Massoli, P., Hildebrandt Ruiz, L., Fortner, E., Williams, L. R., Wilson, K. R., Surratt, J. D., Donahue, N. M., Jayne, J. T., and Worsnop, D. R.: Elemental ratio measurements of organic compounds using aerosol mass spectrometry: characterization, improved calibration, and implications, Atmos. Chem. Phys., 15, 253–272, doi:10.5194/acp-15-253-2015, https://www.atmos-chem-phys.net/15/253/2015/, 2015.

Canonaco, F., Slowik, J. G., Baltensperger, U., and Prévôt, A. S. H.: Seasonal differences in oxygenated organic aerosol composition: implications for emissions sources and factor analysis, Atmos. Chem. Phys., 15, 6993–7002, doi:10.5194/acp-15-6993-2015, 2015.

Cappa, C. D. and Jimenez, J. L.: Quantitative estimates of the volatility of ambient organic aerosol, Atmos. Chem. Phys., 10(12), 5409–5424, doi:10.5194/acp-10-5409-2010, 2010.

Cholakian, A., Beekmann, M., Colette, A., Coll, I., Siour, G., Sciare, J., Marchand, N., Couvidat, F., Pey, J., Gros, V., Sauvage, S., Michoud, V., Sellegri, K., Colomb, A., Sartelet, K., Langley Dewitt, H., Elser, M., Prévôt, A. S. H., Szidat, S., and Dulac, F.: Simulation of organic aerosols in the western Mediterranean area during the ChArMEx 2013 summer campaign, Atmos. Chem. Phys. Discuss., doi:10-51947acp-2017-697, 2017.

Chrit, M., Sartelet, K., Sciare, J., Pey, J., Marchand, N., Couvidat, F., Sellegri, K., and Beekmann, M.: Modelling organic aerosol concentrations and properties during ChArMEx summer campaigns of 2012 and 2013 in the western Mediterranean region, Atmos. Chem. Phys., 17, 12 509–12 531, doi:10.5194/acp-17-12509-2017, 2017.

Ciarelli, G., Aksoyoglu, S., El Haddad, I., Bruns, E. A., Crippa, M., Poulain, L., Äijälä, M., Carbone, S., Freney, E., O'Dowd, C., Baltensperger, U., and Prévôt, A. S. H.: Modelling winter organic aerosol at the European scale with CAMx: valuation and source apportionment with a VBS parameterization based on novel wood burning smog chamber experiments, Atmos. Chem. Phys., 17, 7653–7669, doi:10.5194/acp-17-7653-2017, 2017a.

Ciarelli, G., El Haddad, I., Bruns, E., Aksoyoglu, S., Möhler, O., Baltensperger, U., and Prévôt, A. S. H.: Constraining a hybrid volatility basis-set model for aging of wood-burning emissions using smog chamber experiments: a box-model study based on the VBS scheme of the CAMx model (v5.40), Geosci. Model Dev., 10, 2303–2320, doi:10.5194/gmd-10-2303-2017, 2017b.

Couvidat, F. and Sartelet, K.: The Secondary Organic Aerosol Processor (SOAP v1.0) model: a unified model with different ranges of complexity based on the molecular surrogate approach, Geosci. Model Dev., 8, 1111–1138, doi:10.5194/gmd-8-1111-2015, 2015.

Couvidat, F., Debry, É., Sartelet, K., and Seigneur, C.: A hydrophilic/hydrophobic organic (H^{2}O) model: Model development, evaluation and sensitivity analysis, J. Geophys. Res., 117, D10 304, doi:10.1029/2011JD017214, 2012.

5 Couvidat, F., Kim, Y., Sartelet, K., Seigneur, C., Marchand, N., and Sciare, J.: Modeling secondary organic aerosol in an urban area: application to Paris, France, Atmos. Chem. Phys., 13, 983–996, doi:10.5194/acp-13-983-2013, 2013a.

Couvidat, F., Sartelet, K., and Seigneur, C.: Investigating the impact of aqueous-phase chemistry and wet deposition on organic aerosol formation using a molecular surrogate modeling approach, Environ. Sci. Technol., 47, 914–922, doi:10.1021/es3034318, 2013b.

Couvidat, F., Bessagnet, B., Garcia-Vivanco, M., Real, E., Menut, L., and Colette, A.: Development of an inorganic and organic aerosol model
10 (Chimere2017 β v1.0): seasonal and spatial evaluation over Europe., Geosci. Model Dev. Discuss., in review, doi:doi.org/10.5194/gmd-2017-120, 2017.

Crenn, V., Sciare, J., Croteau, P. L., Verlhac, S., Fröhlich, R., Belis, C. A., Aas, W., Äijälä, M., Alastuey, A., Artiñano, B., Baisnée, D., Bonnaire, N., Bressi, M., Canagaratna, M., Canonaco, F., Carbone, C., Cavalli, F., Coz, E., Cubison, M. J., Esser-Gietl, J. K., Green, D. C., Gros, V., Heikkinen, L., Herrmann, H., Lunder, C., Minguillón, M. C., Močnik, G., O'Dowd, C. D., Ovadnevaite, J., Petit, J.-E., Petralia,
15 E., Poulain, L., Priestman, M., Riffault, V., Ripoll, A., Sarda-Estève, R., Slowik, J. G., Setyan, A., Wiedensohler, A., Baltensperger, U., Prévôt, A. S. H., Jayne, J. T., , and Favez, O.: ACTRIS ACSM intercomparison – Part 1: Reproducibility of concentration and fragment results from 13 individual Quadrupole Aerosol Chemical Speciation Monitors (Q-ACSM) and consistency with co-located instruments, Atmos. Meas. Tech., 8, 5063–5087, doi:10.5194/amt-8-5063-2015, 2015.

Crippa, M., Canonaco, F., Lanz, V., Äijälä, M., Allan, J., Carbone, S., Capes, G., Ceburnis, D., Dall'Osto, M., Day, A., DeCarlo, P., Ehn, M.,
20 Eriksson, A., Freney, E., Hildebrandt Ruiz, L., Hillamo, R., Jimenez, J., Junninen, H., Kiendler-Scharr, A., Kortelainen, A.-M., Kulmala, M., Laaksonen, A., Mensah, A., Mohr, C., Nemitz, E., O'Dowd, C., Ovadnevaite, J., Pandis, S., Petäjä, T., Poulain, L., Saarikoski, S., Sellegri, K., Swietlicki, E., Tiitta, P., Worsnop, D., Baltensperger, U., and Prévôt, A.: Organic aerosol components derived from 25 AMS data sets across Europe using a consistent ME-2 based source apportionment approach., Atmos. Chem. Phys., 14, 6159–6176, doi:10.5194/acp-14-6159-2014, 2014.

25 Dawson, M., Xu, J., Griffin, R., and Dabdub, D.: Development of aroCACM/MPMPO 1.0: a model to simulate secondary organic aerosol from aromatic precursors in regional models., Geosci. Model Dev., 9, 2143–2151, doi:10.5194/gmd-9-2143-2016, 2016.

Debry, É., Fahey, K., Sartelet, K., Sportisse, B., and Tombette, M.: Technical Note: A new SIze REsolved Aerosol Model (SIREAM), Atmos. Chem. Phys., 7, 1537–1547, doi:10.5194/acp-7-1537-2007, 2007.

Denier van der Gon, H. A. C., Bergström, R., Fountoukis, C., Johansson, C., Pandis, S., Simpson, D., and Visschedijk, A.: Particulate
30 emissions from residential wood combustion in Europe: revised estimates and an evaluation, Atmos. Chem. Phys., 15, 6503–6519, doi:10.5194/acp-15-6503-2015, 2015a.

Denier van der Gon, H. A. C., Bergström, R., Fountoukis, C., Johansson, C., Pandis, S. N., Simpson, D., and Visschedijk, A. J. H.: Particulate emissions from residential wood combustion in Europe – revised estimates and an evaluation, Atmos. Chem. Phys., 15, 6503–6519, doi:10.5194/acp-15-6503-2015, 2015b.

35 Donahue, N. M., Robinson, A. L., Stanier, C. O., and Pandis, S. N.: Coupled partitioning, dilution, and chemical aging of semivolatile organics, Environ. Sci. Technol., 40, 2635–2643, doi:10.1021/es052297c, 2006.

Donahue, N. M., Kroll, J. H., Pandis, S. N., and Robinson, A. L.: A two-dimensional volatility basis set – Part 2: Diagnostics of organic-aerosol evolution, Atmos. Chem. Phys., 12, 615–634, doi:10.5194/acp-12-615-2012, 2012.

Duplissy, J., DeCarlo, P. F., Dommen, J., Alfarra, M. R., Metzger, A., Barmpadimos, I., Prévôt, A. S. H., Weingartner, E., Tritscher, T., Gysel, M., Aiken, A. C., Jimenez, J. L., Canagaratna, M. R., Worsnop, D. R., Collins, D. R., Tomlinson, J., and Baltensperger, U.: Relating hygroscopicity and composition of organic aerosol particulate matter, Atmos. Chem. Phys., 11, 1155–1165, doi:10.5194/acp-11-1155-2011, 2011.

El Haddad, I., D'Anna, B., Temime-Roussel, B., Nicolas, M., Boreave, A., Favez, O., Voisin, D., Sciare, J., George, C., Jaffrezo, J.-L., Wortham, H., , and Marchand, N.: Towards a better understanding of the origins, chemical composition and aging of oxygenated organic aerosols: case study of a Mediterranean industrialized environment, Marseille, Atmos. Chem. Phys., 13, 7875–7894, doi:10.5194/acp-13-7875-2013, 2013.

El-Zanan, H., Lowenthal, D., Zielinska, B., Chow, J., and Kumar, N.: Determination of the organic aerosol mass to organic carbon ratio in IMPROVE samples., Chemosphere, 60, 480–496, doi:10.1016/j.chemosphere.2005.01.005, 2005.

ENVIRON: User's Guide, Comprehensive Air Quality Model with Extensions (CAMx), Version 5.40, Environ International Corporation, california, USA, 2011.

Fountoukis, C., Megaritis, A. G., Skyllakou, K., Charalampidis, P. E., Pilinis, C., Denier van der Gon, H. A. C., Crippa, M., Canonaco, F., Mohr, C., Prévôt, A. S. H., Allan, J. D., oulain, L., Petäjä, T., Tiitta, P., Carbone, S., Kiendler-Scharr, A., Nemitz, E., O'Dowd, C., Swietlicki, E., and Pandis, S. N.: Organic aerosol concentration and composition over -Europe: insights from comparison of regional model predictions with aerosol mass spectrometer factor analysis, Atmos. Chem. Phys., 14, 9061–9076, doi:10.5194/acp-14-9061-2014, 2014.

Fröhlich, R., Cubison, M. J., Slowik, J. G., Bukowiecki, N., Canonaco, F., Croteau, P. L., Gysel, M., Henne, S., Herrmann, E., Jayne, J. T., Steinbacher, M., Worsnop, D. R., Baltensperger, U., and Prévôt, A. S. H.: Fourteen months of on-line measurements of the non-refractory submicron aerosol at the Jungfraujoch (3580 m a.s.l.) – chemical composition, origins and organic aerosol sources, Atmos. Chem. Phys., 15, 11 373–11 398, doi:10.5194/acp-15-11373-2015, 2015.

GENEMIS: Technical Report, EUROTEC, annual report 1993, 1994.

Gentner, D., Jathar, S., Gordon, T., Bahreini, R., Day, D., El Haddad, I., Hayes, P., Pieber, S., Platt, S., de Gouw, J., Goldstein, A., Harley, R., Jimenez, J., Prévôt, A., and Robinson, A.: Review of Urban Secondary Organic Aerosol Formation from Gasoline and Diesel Motor Vehicle Emissions, Environ. Sci. Technol., 51, 1074–1093, doi:10.1021/acs.est.6b04509, 2017.

Gilardoni, S., Liu, S., Takahama, S., Russell, L. M., Allan, J. D., Steinbrecher, R., Jimenez, J. L., De Carlo, P. F., Dunlea, E. J., and Baumgardner, D.: Characterization of organic ambient aerosol during MIRAGE 2006 on three platforms, Atmos. Chem. Phys., 9, 5417–5432, doi:10.5194/acp-9-5417-2009, 2009.

Grieshop, A. P., Donahue, N. M., and Robinson, A. L.: Laboratory investigation of photochemical oxidation of organic aerosol from wood fires 2: analysis of aerosol mass spectrometer data, Atmos. Chem. Phys., 9, 2227–2240, doi:10.5194/acp-9-2227-2009, 2009.

Grosjean, D. and Friedlander, S.: Gas-particle distribution factors for organic and other pollutants in the Los Angeles atmosphere., J. Air Pollut. Control Assoc., 25, 1038–1044, 1975.

Guenther, A., Karl, T., Harley, P., Wiedinmyer, C., Palmer, P. I., and Geron, C.: Estimates of global terrestrial isoprene emissions using MEGAN (Model of Emissions of Gases and Aerosols from Nature), Atmos. Chem. Phys., 6, 3181–3210, doi:10.5194/acp-6-3181-2006, 2006.

Hayes, P. L., Carlton, A. G., Baker, K. R., Ahmadov, R., Washenfelder, R. A., Alvarez, S., Rappenglück, B., Gilman, J. B., Kuster, W. C., de Gouw, J. A., Zotter, P., Prévôt, A. S. H., Szidat, S., Kleindienst, T. E., Offenberg, J. H., Ma, P. K., and Jimenez, J. L.: Modeling

the formation and aging of secondary organic aerosols in Los Angeles during CalNex 2010, Atmos. Chem. Phys., 15, 5773–5801, doi:10.5194/acp-15-5773-2015, 2015.

Horowitz, L. W., Walters, S., Mauzerall, D. L., Emmons, L. K., Rasch, P. J., Granier, C., Tie, X., Lamarque, J.-F., Schultz, M. G., Tyndall, G. S., Orlando, J. J., and Brasseur, G. P.: A global simulation of tropospheric ozone and related tracers: Description and evaluation of MOZART, version 2, J. Geophys. Res., 108, 4784, doi:10.1029/2002JD002853, 2003.

Huffman, J. A., Docherty, K. S., Mohr, C., Cubison, M. J., Ulbrich, I. M., Ziemann, P. J., Onasch, T. B., and Jimenez, J. L.: Chemically resolved volatility measurements of organic aerosol from different sources, Environ. Sci. Technol., 43(14), 5351–5357, doi:10.1021/Es803539d, 2009.

Jacobson, M. Z.: Development and application of a new air pollution modeling system – II. Aerosol module structure and design, Atmos. Environ., 31, 131–144, doi:10.1016/1352-2310(96)00202-6, 1997.

Jathar, S. H., Gordon, T. D., Hennigan, C. J., Pye, H. O. T., Pouliot, G., Adams, P. J., Donahue, N. M., and Robinson, A. L.: Unspeciated organic emissions from combustion sources and their influence on the secondary organic aerosol budget in the United States, Proc. Nat. Acad. Sci., 111, 10 473–10 478, doi:10.1073/pnas.1323740111, 2014.

Jimenez, J. L., Canagaratna, M. R., Donahue, N. M., Prevot, A. S., Zhang, Q., Kroll, J. H., DeCarlo, P. F., Allan, J. D., Coe, H., Ng, N. L., Aiken, A. C., Docherty, K. D., Ulbrich, I., Grieshop, A. P., Robinson, A. L., Duplissy, J., Smith, J. D., Wilson, K. R., Lanz, V. A., Hueglin, C., Sun, Y. L., Tian, J., Laaksonen, A., Raatikainen, T., Rautiainen, J., Vaattovaara, P., Ehn, M., Kulmala, M., Tomlinson, J. M., Collins, D. R., Cubison, M. J., Dunlea, E. J., Huffman, J. A., Onasch, T. B., Alfarra, M. R., Williams, P. I., Bower, K., Kondo, Y., Schneider, J., Drewnick, F., Borrmann, S., Weimer, S., Demerjian, K., Salcedo, D., Cottrell, L., Griffin, R., Takami, A., Miyoshi, T., Hatakeyama, S., Shimono, A., Sun, J. Y., Zhang, Y. M., Dzepina, K., Kimmel, J. R., Sueper, D., Jayne, J. T., Herndon, S. C., Trimborn, A. M., Williams, L. R., Wood, E. C., Kolb, C. E., Middlebrook, A. M., Baltensperger, U., and Worsnop, D. R.: Evolution of organic aerosols in the atmosphere, Science, 326, 1525–1529, doi:10.1126/science.1180353, 2009.

Kim, Y., Sartelet, K., and Seigneur, C.: Formation of secondary aerosols: impact of the gas-phase chemical mechanism, Atmos. Chem. Phys., 11, 583–598, doi:10.5194/acp-11-583-2011, 2011.

Kim, Y., Sartelet, K., Seigneur, C., Charron, A., Besombes, J.-L., Jaffrezo, J.-L., Marchand, N., and Polo, L.: Effect of measurement protocol on organic aerosol measurements of exhaust emissions from gasoline and diesel vehicles, Atmos. Environ., 140, 176–187, doi:10.1016/j.atmosenv.2016.05.045, 2016.

Koo, B., Knipping, E., and Yarwood, G.: 1.5-Dimensional volatility basis set approach for modeling organic aerosol in CAMx and CMAQ, Atmos. Environ., 95, 158–164, doi:10.1016/j.atmosenv.2014.06.031, 2014.

Kroll, J. H., Donahue, N. M., Jimenez, J. L., Kessler, S. H., Canagaratna, M., Wilson, K. R., Altieri, K. E., Mazzoleni, L. R., Wozniak, A. S., Bluhm, H., Mysak, E. R., Smith, J. D., E., K. C., and Worsnop, D. R.: Carbon oxidation state as a metric for describing the chemistry of atmospheric organic aerosol, Nature Chem., 3, 133–139, doi:10.1038/NCHEM.948, 2011.

Lipsky, E. M. and Robinson, A. L.: Effects of dilution on fine particle mass and partitioning of semivolatile organics in diesel exhaust and wood smoke, Environ. Sci. Technol., 40(1), 155–162, doi:10.1021/Es050319p, 2006.

May, A. A., Levin, E. J. T., Hennigan, C. J., Riipinen, I., Lee, T., Collett, J. L., Jimenez, J. L., Kreidenweis, S. M., and Robinson, A. L.: Gas-particle partitioning of primary organic aerosol emissions: 3. Biomass burning, J. Geophys. Res.-Atmos., 118, 11 327–11 338, doi:10.1002/jgrd.50828, 2013a.

May, A. A., Levin, E. J. T., Hennigan, C. J., Riipinen, I., Lee, T., Collett Jr., J. L., Jimenez, J. L., Kreidenweis, S. M., and Robinson, A. L.: Gas-particle partitioning of primary organic aerosol emissions: 3. Biomass burning., JournalofGeophysicalResearch, 118, 11 327–11 338, doi:10.1002/jgrd.50828, 2013b.

May, A. A., Presto, A. A., Hennigan, C. J., Nguyen, N. T., Gordon, T. D., and Robinson, A. L.: Gas-particle partitioning of primary organic aerosol emissions: (1) gasoline vehicle exhaust, AtmosphericEnvironment, 77, 128–139, doi:10.1016/j.atmosenv.2013.04.060, 2013c.

May, A. A., Presto, A. A., Hennigan, C. J., Nguyen, N. T., Gordon, T. D., and Robinson, A. L.: Gas-particle partitioning of primary organic aerosol emissions: (2) diesel vehicles, EnvironmentalScienceandTechnology, 47, 8288–8296, doi:10.1021/es400782j, 2013d.

Michoud, V., Sciare, J., Sauvage, S., Dusanter, S., Léonardis, T., Gros, V., Kalogridis, C., Zannoni, N., Féron, A., Petit, J.-E., Crenn, V., Baisnée, D., Sarda-Estève, R., Bonnaire, N., Marchand, N., DeWitt, H., Pey, J., Colomb, A., Gheusi, F., Szidat, S., Stavroulas, I., Borbon, A., and Locoge, N.: Organic carbon at a remote site of the western Mediterranean Basin: sources and chemistry during the ChArMEx SOP2 field experiment, Atmos. Chem. Phys., 17, 8837–8865, doi:10.5194/acp-17-8837-2017, 2017.

Minguillón, M., Pérez, N., Marchand, N., Bertrand, A., Temime-Roussel, B., Agrios, K., Szidat, S., van Drooge, B., Sylvestre, A., Alastuey, A., Reche, C., Ripoll, A., Marco, E., Grimalt, J., and Querol, X.: Secondary organic aerosol origin in an urban environment: influence of biogenic and fuel combustion precursors, Faraday Discuss., 189, 337–359, doi:10.1039/c5fd00182j, 2016.

Molteni, U., Bianchi, F., Klein, F., El Haddad, I., Frege, C., Rossi, M., Dommen, J., , and Baltensperger, U.: Formation of highly oxygenated organic molecules from aromatic compounds., Atmos. Chem. Phys., doi:10.5194/acp-2016-1126, 2018.

Murphy, B., Woody, M., Jimenez, J., Carlton, A., Hayes, P., Liu, S., Ng, N., Russell, L., Setyan, A., Xu, L., Young, J., Zaveri, R., Zhang, Q., and Pye, H.: Semivolatile POA and parameterized total combustion SOA in CMAQv5.2: impacts on source strength and partitioning., Atmos. Chem. Phys., 17, 11 107–11 133, doi:10.5194/acp-17-11107-2017, 2017.

Murphy, D. M., Cziczo, D. J., Froyd, K. D., Hudson, P. K., Matthew, B. M., Middlebrook, A. M., Peltier, R. E., Sullivan, A., Thomson, D. S., and Weber, R. J.: Single-particle mass spectrometry of tropospheric aerosol particles, J. Geophys. Res., 11, 23–32, doi:10.1029/2006JD007340, 2006.

Nenes, A., Pandis, S. N., and Pilinis, C.: ISORROPIA: A new thermodynamic equilibrium model for multiphase multicomponent inorganic aerosols, Aquat. Geochem., 4, 123–152, doi:10.1023/A:1009604003981, 1998.

Ng, N. L., Herndon, S. C., Trimborn, A., Canagaratna, M. R., Croteau, P. L., Onasch, T. B., Sueper, D., Worsnop, D. R., Zhang, Q., Sun, Y. L., and Jayne, J. T.: An Aerosol Chemical Speciation Monitor (ACSM) for Routine Monitoring of the Composition and Mass Concentrations of Ambient Aerosol, Aerosol Sci. Technol., 45, 780–794, doi:10.1080/02786826.2011.560211, 2011.

Nicolas, J.: Caractérisation physico-chimique de l'aérosol troposphérique en Méditerranée : sources et devenir, PhD dissertation, Univ. Versailles-Saint-Quentin-en-Yvelines, 2013.

Ots, R., Young, D., Vieno, M., Xu, L., Dunmore, R., Allan, J., Coe, H., Williams, L., Herndon, S., Ng, N., Hamilton, J., Begström, R., Di Marco, C., Nemitz, E., Mackenzie, I., Kuenen, J., Green, D., Reis, S., and Heal, M.: Simulating secondary organic aerosol from missing diesel-related intermediate-volatility organic compound emissions during the Clean Air for London (ClearfLo) campaign., Atmos. Chem. Phys., 16, 6453–6473, doi:10.5194/acp-16-6453-2016, 2016.

Robinson, A. L., Donahue, N. M., Shrivastava, M. K., Weitkamp, E. A., Sage, A. M., Grieshop, A. P., Lane, T. E., Pierce, J. R., and Pandis, S. N.: Rethinking Organic Aerosols: Semivolatile Emissions and Photochemical Aging, Science, 315, 1259–1262, doi:10.1126/science.1133061, 2007.

Sartelet, K., Couvidat, F., Seigneur, C., and Roustan, Y.: Impact of biogenic emissions on air quality over Europe and North America, Atmos. Environ., 53, 131–141, 2012.

Sartelet, K., Zhu, S., Moukhtar, S., André, M., André, J. M., Gros, V., Favez, O., Brasseur, A., and Redaelli, M.: Emission of intermediate, semi and low volatile organic compounds from traffic and their impact on secondary organic aerosol concentrations over Greater Paris, Atmos. Environ., 180, 126–137, doi:10.1016/j.atmosenv.2018.02.031, 2018.

Sartelet, K. N., Debry, E., Fahey, K., Roustan, Y., Tombette, M., and Sportisse, B.: Simulation of aerosols and related species over Europe with the Polyphemus system. Part I: model-to-data comparison for 2001, Atmos. Environ., 41, 6116–6131, doi:10.1016/j.atmosenv.2007.04.024, 2007.

Schwier, A. N., Rose, C., Asmi, E., Ebling, A. M., Landing, W. M., Marro, S., Pedrotti, M.-L., Sallon, A., Iuculano, F., Agusti, S., Tsiola, A., Pitta, P., Louis, J., Guieu, C., Gazeau, F., , and Sellegri, K.: Primary marine aerosol emissions from the Mediterranean Sea during pre-bloom and oligotrophic conditions: correlations to seawater chlorophyll a from a mesocosm study, Atmos. Chem. Phys., pp. 7961–7976, doi:10.5194/acp-15-7961-2015, 2015.

Shrivastava, M., Cappa, C., Fan, J., Goldstein, A., Guenther, A., Jimenez, J., Kuang, C., Laskin, A., Martin, S., Ng, N., Petaja, T., Pierce, J., Rasch, P., Roldin, P., Seinfeld, J., Shilling, J., Smith, J., Thornton, J., Volkamer, R., Wang, J., Worsnop, D., Zaveri, R., Zelenyuk, A., and Zhang, Q.: Recent advances in understanding secondary organic aerosol: Implications for global climate forcing, Rev. Geophys., 55, 509–559, doi:10.1002/2016RG000540, 2017.

Stockwell, C. E., Veres, P. R., Williams, J., and Yokelson, R. J.: Characterization of biomass burning emissions from cooking fires, peat, crop residue, and other fuels with high-resolution proton-transfer-reaction time-of-flight mass spectrometry, Atmos. Chem. Phys., 15, 845–865, doi:10.5194/acp-15-845-2015, 2015.

Tost, H. and Pringle, K. J.: Improvements of organic aerosol representations and their effects in large-scale atmospheric models, Atmos. Chem. Phys., 12, 8687–8709, doi:10.5194/acp-12-8687-2012, 2012.

Troen, I. B. and Mahrt, L.: A simple model of the atmospheric boundary layer; sensitivity to surface evaporation, Bound.-Layer Meteorol., 37, 129–148, doi:10.1007/BF00122760, 1986.

Tsimpidi, A. P., Karydis, V. A., Zavala, M., Lei, W., Molina, L., Ulbrich, I. M., Jimenez, J. L., and Pandis, S. N.: Evaluation of the volatility basis-set approach for the simulation of organic aerosol formation in the Mexico City metropolitan area, Atmos. Chem. Phys., 10, 525–546, doi:10.5194/acp-10-525-2010, 2010.

Tsimpidi, A. P., Karydis, V. A., Pandis, S. N., and Lelieveld, J.: Global-scale combustion sources of organic aerosols: sensitivity to formation and removal mechanisms, Atmos. Chem. Phys., 17, 7345–7364, doi:10.5194/acp-17-7345-2017, 2017.

Tsimpidi, A. P., Karydis, V. A., Pozzer, A., Pandis, S. N., and Lelieveld, J.: ORACLE 2-D (v2.0): an efficient module to compute the volatility and oxygen content of organic aerosol with a global chemistry–climate model, Geosci. Model Dev., 11, 3369–3389, doi:10.5194/gmd-11-3369-2018, https://www.geosci-model-dev.net/11/3369/2018/, 2018.

Turpin, B. and Lim, H.-J.: Species Contributions to PM2.5 Mass Concentrations: Revisiting Common Assumptions for Estimating Organic Mass., Aerosol Sci. Technol., 35, 602–610, doi:10.1080/02786820119445, 2001.

Wong, J. P. S., Lee, A. K. Y., Slowik, J. G., Cziczo, D. J., Leaitch, W. R., Macdonald, A., and Abbatt, J. P. D.: Oxidation of ambient biogenic secondary organic aerosol by hydroxyl radicals: Effects on cloud condensation nuclei activity, Geophys. Res. Lett., 38, 22 805–22 811, doi:10.1029/2011GL04935, 2011.

Woody, M. C., Baker, K. R., Hayes, P. L., Jimenez, J. L., Koo, B., and Pye, H. O. T.: Understanding sources of organic aerosol during CalNex-2010 using the CMAQ-VBS, Atmos. Chem. Phys., 16, 4081–4100, doi:10.5194/acp-16-4081-2016, 2016.

Xing, L., Fu, T.-M., Cao, J. J., Lee, S. C., Wang, G. H., Ho, K. F., Cheng, M.-C., You, C.-F., and Wang, T. J.: Seasonal and spatial variability of the OM/OC mass ratios and high regional correlation between oxalic acid and zinc in Chinese urban organic aerosols, Atmos. Chem. Phys., 13, 4307–4318, doi:10.5194/acp-13-4307-2013, 2013.

Zhang, Q., Alfarra, M., Worsnop, D., Allan, J., Coe, H., Canagaratna, M., and Jimenez, J.: Deconvolution and quantification of hydrocarbon-like and oxygenated organic aerosols based on aerosol mass spectrometry., Environ. Sci. Technol., 39, 4938–4952, doi:10.1021/es048568l, 2005a.

Zhang, Q., Worsnop, D., Canagaratna, M., and Jimenez, J.: Hydrocarbon-like and oxygenated organic aerosols in Pittsburgh: insights into sources and processes of organic aerosols., Atmos. Chem. Phys., 5, 3289–3311, doi:10.5194/acp-5-3289-2005, 2005b.

Zhao, Y., Nguyen, N., Presto, A., Hennigan, C., May, A., and Robinson, A.: Intermediate volatility organic compound emissions from on-road diesel vehicles: chemical composition, emission factors, and estimated secondary organic aerosol production., Environ. Sci. Technol., 49, 11 516–11 526, doi:10.1021/acs.est.5b02841, 2015.

Zhao, Y., Nguyen, N., Presto, A., Hennigan, C., May, A., and Robinson, A.: Intermediate volatility organic compound emissions from on-road gasoline vehicles and small off-road gasoline engines., Environ. Sci. Technol., 50, 4554–4563, doi:10.1021/acs.est.5b06247, 2016.

Zhu, S., Sartelet, K., Healy, R., and Wenger, J.: Simulation of particle diversity and mixing state over Greater Paris: A model-measurement inter-comparison, Faraday Discuss., 189, 547–566, doi:10.1039/C5FD00175G, 2016.

Appendix A: Statistical indicators and criteria

Statistic indicator	Definition
Root mean square error (RMSE)	$\sqrt{\frac{1}{n}\sum_{i=1}^{n}(c_i - o_i)^2}$
Correlation (Corr)	$\dfrac{\sum_{i=1}^{n}(c_i - \bar{c})(o_i - \bar{o})}{\sqrt{\sum_{i=1}^{n}(c_i - \bar{c})^2}\sqrt{\sum_{i=1}^{n}(o_i - \bar{o})^2}}$
Mean fractional bias (MFB)	$\frac{1}{n}\sum_{i=1}^{n}\dfrac{c_i - o_i}{(c_i + o_i)/2}$
Mean fractional error (MFE)	$\frac{1}{n}\sum_{i=1}^{n}\dfrac{\mid c_i - o_i \mid}{(c_i + o_i)/2}$

Table A1. Definitions of the statistics used in this work. $(o_i)_i$ and $(c_i)_i$ are the observed and the simulated concentrations at time and location i, respectively. n is the number of data

Criteria	Performance criterion	Goal criterion
|MFB|	$\leq 60\%$	$\leq 30\%$
MFE	$\leq 75\%$	$\leq 50\%$

Table A2. Boylan and Russel criteria

Appendix B: Single-step ageing of I/S-VOCs (Couvidat et al., 2012)

$$POAlP + OH \xrightarrow{k} SOAlP \tag{B1}$$

$$POAmP + OH \xrightarrow{k} SOAmP \tag{B2}$$

$$POAhP + OH \xrightarrow{k} SOAhP \tag{B3}$$

$$\tag{B4}$$

with k = 2.0×10^{-11} cm^3. molecule^{-1}. s^{-1}.

Surrogate	Emission fraction	Molecular weight	$\log_{10}(C^*)$ at 298K	ΔH_{vap}	OM/OC	O/C
POAlP	0.25	280	-0.04	106.0	1.3	0.15
POAmP	0.32	280	1.94	91.0	1.3	0.15
POAhP	0.43	280	3.51	79.0	1.3	0.15
SOAlP	—	392	-2.04	106.0	1.82	0.56
SOAmP	—	392	-0.06	91.0	1.82	0.56
SOAhP	—	392	1.51	79.0	1.82	0.56

Table B1. Properties of the primary and secondary anthropogenic I/S-VOCs. The molecular weights are in g.mol^{-1}. ΔH_{vap} is the enthalpy of vaporisation in KJ.mol^{-1}, which describes the temperature dependance of the saturation pressure C*.

Appendix C: Multi-step ageing of I/S-VOCs (Koo et al., 2014)

$$VAP1 + OH \xrightarrow{k} 0.864VAP0 + 0.142VAS0 \tag{C1}$$

$$VAP2 + OH \xrightarrow{k} 0.877VAP1 + 0.129VAS1 \tag{C2}$$

$$VAP3 + OH \xrightarrow{k} 0.889VAP2 + 0.116VAS2 \tag{C3}$$

$$VAP4 + OH \xrightarrow{k} 0.869VAP3 + 0.137VAS3 \tag{C4}$$

$$\tag{C5}$$

with k = 4.0×10^{-11} cm^3. molecule^{-1}. s^{-1}.

Surrogate	Emission fraction	Molecular weight	$\log_{10}(C^*)$ at 298K	ΔH_{vap}	OM/OC	O/C
VAP0	0.15	278	-1	96.0	1.36	0.16
VAP1	0.20	275	0	85.0	1.31	0.12
VAP2	0.31	272	1	74.0	1.26	0.07
VAP3	0.20	268	2	63.0	1.21	0.03
VAP4	0.14	266	3	55.0	1.17	0.00
VAS0	—	172	-1	35	2.05	0.70
VAS1	—	167	0	35	1.92	0.60
VAS2	—	163	1	35	1.81	0.51
VAS3	—	158	2	35	1.70	0.43
VAS4	—	153	3	35	1.59	0.34

Table C1. Properties of the VBS species (the primary and secondary anthropogenic SVOCs). The molecular weights are in g.mol^{-1}. ΔH_{vap} is the enthalpy of vaporisation in KJ.mol^{-1}, which describes the temperature dependance of the saturation pressure C*.

Appendix D: Multi-step ageing of I/S-VOCs from residential heating (Ciarelli et al., 2017b)
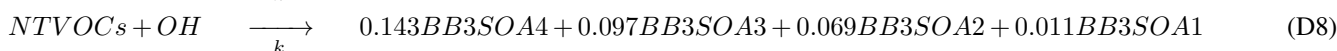
$$BBPOA4 + OH \xrightarrow{k} BBSOA3 \tag{D1}$$

$$BBPOA3 + OH \xrightarrow{k} BBSOA2 \tag{D2}$$

$$BBPOA2 + OH \xrightarrow{k} BBSOA1 \tag{D3}$$

$$BBPOA1 + OH \xrightarrow{k} BBSOA0 \tag{D4}$$

$$BBSOA3 + OH \xrightarrow{k} BBSOA2 \tag{D5}$$

$$BBSOA2 + OH \xrightarrow{k} BBSOA1 \tag{D6}$$

$$BBSOA1 + OH \xrightarrow{k} BBSOA0 \tag{D7}$$

$$NTVOCs + OH \xrightarrow{k} 0.143BB3SOA4 + 0.097BB3SOA3 + 0.069BB3SOA2 + 0.011BB3SOA1 \tag{D8}$$

$$BB3SOA4 + OH \xrightarrow{k} BB3SOA3 \tag{D9}$$

$$BB3SOA3 + OH \xrightarrow{k} BB3SOA2 \tag{D10}$$

$$BB3SOA2 + OH \xrightarrow{k} BB3SOA1 \tag{D11}$$

$$BB3SOA1 + OH \xrightarrow{k} BB3SOA0 \tag{D12}$$

$$\tag{D13}$$

with k = 4.0×10^{-11} cm^3. molecule^{-1}. s^{-1}.

Surrogate	Emission fraction	Molecular weight	$\log_{10}(C^*)$ at 298K	ΔH_{vap}	OM/OC	O/C
NTVOCs	4.75	113	6	—	—	—
BBPOA0	0.20	216	-1	85.0	1.64	0.37
BBPOA1	0.10	216	0	77.5	1.53	0.29
BBPOA2	0.10	216	1	70.0	1.44	0.22
BBPOA3	0.20	216	2	62.5	1.36	0.15
BBPOA4	0.40	215	3	55.0	1.28	0.09
BBSOA0	—	194	-1	35.0	1.80	0.50
BBSOA1	—	189	0	35.0	1.70	0.43
BBSOA2	—	184	1	35.0	1.61	0.36
BBSOA3	—	179	2	35.0	1.53	0.29
BB3SOA0	—	149	-1	35.0	2.48	1.05
BB3SOA1	—	144	0	35.0	2.29	0.90
BB3SOA2	—	140	1	35.0	2.12	0.76
BB3SOA3	—	135	2	35.0	1.96	0.63
BB3SOA4	—	131	3	35.0	1.82	0.52

Table D1. Properties of the VBS species (the NTVOCs and primary and secondary RH-I/S-VOCs). The molecular weights are in g.mol^{-1}. ΔH_{vap} is the enthalpy of vaporisation in KJ.mol^{-1}, which describes the temperature dependance of the saturation pressure C*.

Appendix E: Maps of OM$_1$ concentrations and differences between simulations.
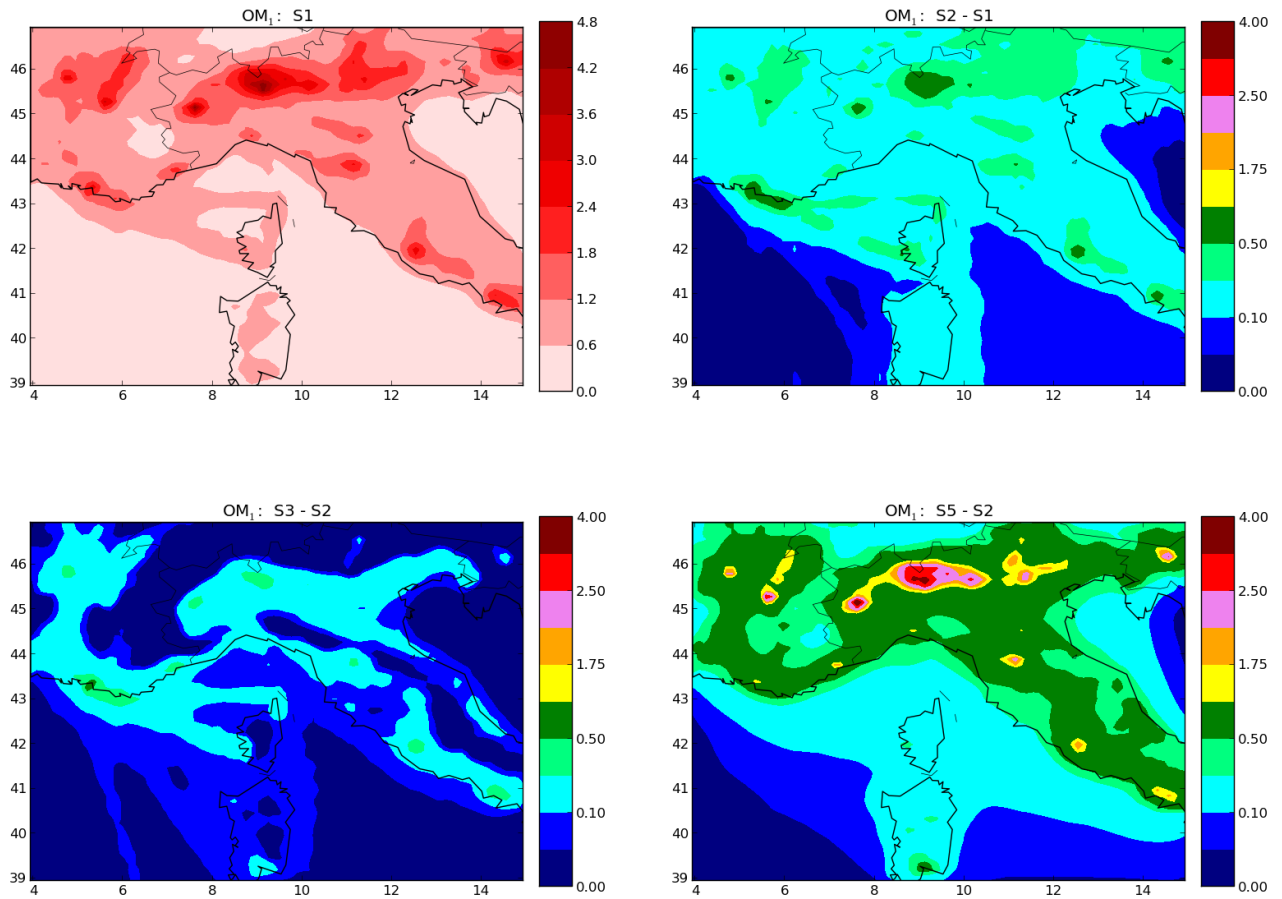
Figure E1. Maps of the concentrations of OM_1 ($\mu g\,m^{-3}$) averaged over January to March 2014 using S1 (upper left panel) and the absolute difference of OM_1 concentrations between S2 and S1 (upper right panel, impact of volatility), S3 and S2 (lower left panel, impact of multi-step ageing), and S5 and S2 (lower right panel, impact of increasing R_{RH} from 1.5 to 4.